Clim. Past Discuss., doi:10.5194/cp-2017-49, 2017
Manuscript under review for journal Clim. Past
Discussion started: 15 May 2017

Climate of the Past Discussions

Atlantic Multidecadal Variability from the Last Millennium Reanalysis

Hansi K. A. Singh[1], Gregory J. Hakim[2], Robert Tardif[2], Julien Emile-Geay[3], and David C. Noone[4]

[1]Pacific Northwest National Laboratory, US Department of Energy, Richland WA USA
[2]Department of Atmospheric Sciences, University of Washington, Seattle WA USA
[3]Department of Earth Sciences, University of Southern California, Los Angeles CA USA
[4]College of Earth, Ocean, and Atmospheric Sciences, Corvallis OR USA

Correspondence to: Hansi K.A. Singh (hansi.singh@pnnl.gov)

Abstract. The Last Millennial Reanalysis (LMR) employs a data assimilation approach to reconstruct climate fields from annually-resolved proxy data over years 0-2000CE. We use the LMR to examine Atlantic Multidecadal Variability (AMV) over the last two millennia, and find several robust thermodynamic features associated with a positive Atlantic Multidecadal Oscillation (AMO) index that reveal a dynamically-consistent pattern of variability: the Atlantic and most continents warm; sea ice thins over the Arctic and retreats over the Greenland-Iceland-Norwegian Seas; and equatorial precipitation shifts northward. The latter is consistent with anomalous southward energy transport mediated by the atmosphere. Net downward shortwave radiation increases at both the top-of-atmosphere and surface, indicating a decrease in planetary albedo, likely due to a decrease in low clouds. Heat is absorbed by the climate system and the oceans warm. Wavelet analysis of the AMV time series shows a reddening of the frequency spectrum at the 50-to-100-year time scale, but no evidence of a distinct multidecadal or centennial spectral peak. This latter result is insensitive to both choice of prior model and calibration dataset used in the data assimilation algorithm, suggesting that the lack of a distinct multidecadal spectral peak is a robust result.

1 Introduction

Modeling and observational studies have shown that north Atlantic sea surface temperatures (SSTs) co-vary with precipitation over the African Sahel (Zhang and Delworth, 2006), Eurasia (R. Lu and Ding, 2006; Zhang and Delworth, 2006), and North America (Enfield et al., 2001); hurricane development and intensity over the Atlantic (Zhang and Delworth, 2006); drought over the North American interior (McCabe et al., 2004; Nigam et al., 2011); summer temperatures over Europe and the Americas (Sutton and Hodson, 2005); sea ice thickness and extent over the Arctic (Miles et al., 2014); climate variability over the Pacific (Dong et al., 2006); and marine primary productivity (Henson et al., 2009). Improved prediction of global climate perturbations likely depends on better understanding of north Atlantic variability.

Kushnir (1994) shows that north Atlantic sea surface temperatures (SSTs) appear to vary at both interannual and interdecadal time scales, and that variability at these different time scales is substantively different. While wind and surface pressure appear to covary with north Atlantic SSTs at short time scales, longer time scale variability appears to be uncorrelated with these fields. Kushnir (1994) concludes that these different time scales constitute different phenomena, and suggests that the longer

Clim. Past Discuss., doi:10.5194/cp-2017-49, 2017
Manuscript under review for journal Clim. Past
Discussion started: 15 May 2017

time scale portion of the variability could be driven by ocean-atmosphere coupling. This longer time scale variability is known today as the Atlantic Multidecadal Oscillation (AMO) or Atlantic Multidecadal Variability (AMV).

Studies of the observational and paleoproxy records provide evidence of multidecadal variability centered over the Atlantic. The Central England Temperature record, the longest observational temperature time series, suggests a 65-year time scale of variability over the last 350 years (Tung and Zhou, 2013). Evidence of multidecadal Atlantic variability (with time scales anywhere between 20 and 80 years) has also been found in proxy tree ring records (Delworth and Mann, 2000; Gray et al., 2004), annually-resolved ice cores (Chylek et al., 2011), and coral isotope records (Hetzinger et al., 2008). Lengthy proxy records extending over the last 8000 years also show multidecadal spectral power, though this power is not stationary over space or time (Knudsen et al., 2011).

Many studies have explored ocean-atmosphere interactions as driving factors for AMV, with changes in SSTs in the North Atlantic controlled by natural (unforced) fluctuations in the Atlantic meridional overturning circulation (AMOC) (see, e.g., Delworth et al., 1993; Polyakov et al., 2005; Zhang et al., 2007). Several dynamical studies have suggested that zonal and meridional oscillations in the AMOC on multidecadal time scales may drive changes in north Atlantic SSTs (Dijkstra et al., 2006, 2008). While long-term observational records of the AMOC state are unavailable, observational evidence of sea surface height appear to support the idea that north Atlantic SSTs co-vary with changes in sea surface height along the eastern seaboard of the United States, which is consistent with changes in the AMOC (McCarthy et al., 2015).

Nevertheless, there remains disagreement regarding the role of AMOC changes in driving north Atlantic SST variability over multidecadal time scales. Tandon and Kushner (2015) show that the relationship between AMV and the AMOC may not be stationary between the preindustrial and industrial periods: while AMOC fluctuations appeared to lead changes in north Atlantic SSTs over the preindustrial period in models, this lead-lag relationship reversed during the industrial era with strong anthropogenic forcing of the climate system. Recently, Clement et al. (2015) show that stochastic coupling between the atmosphere and oceanic mixed layer is sufficient to recover the AMV found in most climate models, calling into question the role of the oceanic MOC as a driver of AMV. Indeed, only some state-of-the-art global climate models (GCMs) simulate multidecadal variability in Atlantic SSTs (Clement et al., 2015), while one older GCM has been shown to display spurious multidecadal variability due to poor parameterization of ocean mixing processes (see Danabasoglu, 2008). Hakkinen et al. (2011) suggest that changes in the strength of the north Atlantic subpolar and subtropical gyres may be more closely linked to AMV than variations in the AMOC; such multidecadal shifts in the gyres alter atmospheric blocking patterns which may, in turn, perturb SSTs over the entire Atlantic basin.

The role of aerosols as external drivers of north Atlantic SST variability has also been debated. Aerosol release by volcanic eruptions has been suggested to act as an external driver of AMV in the preindustrial period (Ottera et al., 2010; Knudsen et al., 2014), contrary to other studies that suggest that AMV is internally-driven by ocean-atmosphere interactions. Over the industrial period, the role of anthropogenic aerosols in driving AMV also remains an open question. Booth et al. (2012) argue that aerosol direct and indirect effects over the modern era (post-1850) have strongly impacted multidecadal SST variability over the north Atlantic, resulting in an evolution of north Atlantic SSTs that mimic an internally-driven oscillation. This argument, however, has been challenged by Zhang et al. (2013), who suggest that the GCM used in Booth et al. (2012)

Clim. Past Discuss., doi:10.5194/cp-2017-49, 2017
Manuscript under review for journal Clim. Past
Discussion started: 15 May 2017

incorrectly modeled aerosol effects, and show that improved representation of these effects reveals that 20th century surface temperature variations can not be explained in full by changes in anthropogenic aerosol emissions.

Given major disagreements between climate models in AMV representation, it's clear that study of AMV dynamics would benefit from using observational data from the real Earth system. However, detailed study of AMV has been severely limited by the brevity of the instrumental record, which is less than two centuries long. Furthermore, these observations are from a time period characterized by intense anthropogenic forcing of the climate system through greenhouse gases, aerosols, land use changes, ozone-depleting substances, and others. While the instrumental record is short and likely biased towards a forced response, the proxy record does not suffer from this shortcoming. Indeed, annually-resolved proxies for temperature from tree rings, corals, ice cores, and others, exist at annual resolution over the last several millennia. Although proxy records exist over much longer periods than observations, an objective procedure for assimilating these proxies into coherent spatial fields remains an ongoing challenge.

The Last Millennial Reanalysis (LMR) provides a robust framework for such objective assimilation of proxies for the reconstruction of spatial fields (Hakim et al., 2016). In this study, we use climate field reconstructions made possible by the LMR to analyze the climate dynamics of AMV. By assimilating temperature-dependent information from proxy records, we consider what thermodynamic features characterize AMV over the last 2000 years, and whether these features have changed with time, particularly between the preindustrial (yrs 0 to 1850) and modern (yrs 1850 to 2000) eras. Since the data assimilation procedure used in the LMR relies on the use of a prior dataset (as described in Steiger et al., 2014; Hakim et al., 2016), we will also note what additional information assimilation of proxies yields beyond that found in this prior dataset. Finally, we will use the LMR to consider what, if any, robust time scales characterize AMV over the last two millennia, and how these time scales computed from assimilation of the observations compare to those found in previous studies.

The remainder of this paper is organized as follows. We describe the LMR proxy assimilation and climate field reconstruction procedure, along with details of our regression and time scale analysis methodologies in §2. In §3.1, we consider the AMO index over the last 2000 years, as inferred from the LMR, and in §3.2, we describe the basic climate state that corresponds to a positive AMO index. We highlight the energetics associated with a positive AMO index in §3.3, particularly top-of-atmosphere and surface fluxes, the implied meridional energy transports, and flux imbalances. In §3.4, we consider time scales of AMV using wavelet analysis. We conclude by discussing our findings, their implications, and caveats of our approach in §4.

2 Methods

The climate field reconstruction methodology used in the LMR is described in detail by Steiger et al. (2014) and is validated for temperature reconstructions over the modern era (yrs 1850 to 2000 CE) in Hakim et al. (2016). In brief, the data assimilation procedure updates the state of the prior, $\boldsymbol{x}_p$ to some new state $\boldsymbol{x}_a$ using information from the proxies $\boldsymbol{y}$ that is weighted using a Kalman gain matrix $\mathbf{K}$:

$$\boldsymbol{x}_a = \boldsymbol{x}_p + \mathbf{K}(\boldsymbol{y} - \mathcal{H}(\boldsymbol{x}_p))\ . \tag{1}$$

Clim. Past Discuss., doi:10.5194/cp-2017-49, 2017
Manuscript under review for journal Clim. Past
Discussion started: 15 May 2017

Climate of the Past Discussions Open Access EGU

Here, $\mathcal{H}$ is the observation model that converts the prior state to its proxy equivalent, $\mathcal{H}(\boldsymbol{x}_p)$. The innovation, $\boldsymbol{y} - \mathcal{H}(\boldsymbol{x}_p)$, contains new information from the observations that is not already present in the prior. The Kalman gain matrix $\mathbf{K}$, which weights the innovation and maps from proxy space to physical space, is

$$\mathbf{K} = \mathbf{B}\mathbf{H}^{\mathbf{T}}(\mathbf{H}\mathbf{B}\mathbf{H}^{\mathbf{T}} + \mathbf{R})^{-1} \tag{2}$$

where $\mathbf{B}$ is the error covariance matrix for the prior data (computed as the sample mean of $\boldsymbol{x}_p$), $\mathbf{H}$ is the linearization of the observation model $\mathcal{H}$ about the prior mean, and $\mathbf{R}$ is the error covariance matrix for the proxies (described further below). The numerator of matrix $\mathbf{K}$, $\mathbf{B}\mathbf{H}^{\mathbf{T}}$, is the covariance expectation between the prior and the prior-estimated observations, and acts to spread information from proxy locales into the physical space.

The observation model $\mathbf{H}$, a forward model which maps from physical space to the proxy space, is constructed using a calibration dataset and assumes a linear relationship between the proxy state and temperature over the calibration period:

$$y = \beta_0 + \beta_1 T' + \epsilon \tag{3}$$

where T' is the annual-mean 2-m air temperature anomaly from the calibration dataset, β_0 is the intercept, β_1 is the slope, and ϵ is a Gaussian random variable with zero mean and a variance of σ^2. The calibration temperature T' for a given proxy record is chosen from the gridpoint closest to the proxy location at concurrent time periods, and parameters β_0, β_1, and σ are computed using a linear least-squares fit during the time period 1900-2000. The diagonal elements of $\mathbf{R}$, the error covariance matrix for the proxies, are the variance of the regression residuals, σ^2.

The state $\boldsymbol{x}_a$ is computed 'offline' for each year (i.e. each year is computed independently) between 1 to 2000 CE. The proxies used are a total of 465 timeseries from the PAGES2K dataset (Consortium, 2013; Hakim et al., 2016), which includes lake sediment calcium to phosphorus ratios, ice core water isotopes (both oxygen and hydrogen), coral oxygen isotopes, tree rings (width and density), and speleothem water isotopes. As described in Hakim et al. (2016), the LMR reconstructions of temperature and 500 hPa geopotential height have been validated by comparison to other reanalysis datasets over the modern era.

The reanalysis used here is performed using the Community Climate System Model version 4 (CCSM4) Last Millenium run (from Phase 5 of the Climate Model Intercomparison Project) as the prior $\boldsymbol{x}_p$. The calibration dataset for creating the observation model is the NOAA Merged Land-Ocean Surface Temperature Analysis (MLOST; Smith et al., 2008). Though the reanalysis results obtained when using different prior and calibration datasets are quantitatively distinct (see Figure 12 in Hakim et al., 2016), they all yield qualitatively similar results. Therefore, much of the ensuing analysis, apart from calculation of time scales (see below), is performed using this single reanalysis, hereafter referred to as MLOST-CCSM4.

Following Clement et al. (2015) and others, we quantify AMV using the AMO index, which is computed annually as the average of the area-weighted SSTs from 60N to the equator and 120W to the prime meridian. Links between climate variables and AMV are defined by regression onto the AMO index and computing the value of the variable at two standard deviations of the AMO index. In order to isolate multidecadal (and longer) time scale variability, both the AMO index and variable fields are filtered using a 20-year low-pass Lanczos filter with 31 filter weights prior to computing the regressions (unless otherwise noted). The AMO index and climate variable fields are detrended before regression. Regression results from the LMR are computed for three time periods to highlight potential non-stationarity in AMV: years 0 to 1850 (the preindustrial era), 1200 to 1850 (the part of the preindustrial era when proxy coverage is substantial), and 1850 to 2000 (the industrial era). These results are compared to similar results from the CCSM4 prior.

AMV time scale analysis was performed with wavelets using the methodology described by Torrence and Compo (1998). The Paul wavelet is used with a scale spacing of 0.25 and a total of 52 scales. Significance is computed at $p < 0.05$, using a one-step autoregression (AR(1); i.e. red noise) process as the null hypothesis; significance results were found to be insensitive to choice of the mother wavelet. Wavelet analysis was performed on six different AMO index reconstructions using 2 different priors and 3 different calibration datasets (see Table 1).

Prior Datasets		
Name	Acronym	Reference
Community Climate System Model, version 4 CMIP5 Last Millenium Run	CCSM4 (default)	Landrum et al. (2012)
Max Planck Institute Earth System Model, paleo-mode CMIP5 Last Millenium Run	MPI	Jungclaus et al. (2010)
Calibration Dataset		
Name	Acronym	Reference
NOAA Merged Land-Ocean Surface Temperature Analysis, version 3.5.4	MLOST (default)	Smith et al. (2008)
NASA Goddard Institute for Space Studies Surface Temperature Analysis	GIS	Hansen et al. (2010)
Met Office Hadley Centre Climate Research Unit Temperature, version 4.4.0.0	CRU	Morice et al. (2012)

Table 1. Prior and calibration datasets used in the LMR reconstruction. The default datasets are used for all analyses, while additional datasets are only used in the wavelet time scale analyses.

3 Results

3.1 The AMO index in the LMR

Over the last 2000 years, the AMO index reconstructed from the LMR resembles the global mean surface temperature (GMST) timeseries (Figures 1a and b, respectively; $r = 0.97$ at lag 0). Like the GMST, the AMO has the least variability over the first 1000 years of the reanalysis, possibly due to the lack of globally-distributed proxy records over this early period of the reanalysis. Over the latter portion of the reanalysis (year 900 CE forward), a cooling trend is evident in both the AMO and GMST, which is punctuated by a warmer period centered at year 1500 CE. A warming trend is evident in both the AMO and GMST timeseries following year 1900 CE.

In Figure 1c, we show the LMR reconstruction of the AMO index over years 1900 to 2000 CE, along with three different reanalysis datasets: NASA's GIStemp, ERA-20C, and the 20CR. Comparison with these other reanalyses suggests that the LMR MLOST-CCSM4 reconstruction reasonably re-creates the the north Atlantic SST record over the last century: as expected, the LMR and the three reanalyses all show an upward trend in the AMO index over this time period, and all reveal intermittent periods of rapid and slower temperature rise, suggesting a multi-decadal oscillation. The LMR displays slightly weaker amplitude in this multi-decadal timescale than the other reanalyses. We return to this question of timescales in §3.4.

3.2 Thermodynamics of AMV in the LMR

Globally, the temperature field associated with a positive AMO index is characterized by warming over the continents and especially strong warming over the far northern reaches of the Atlantic and Arctic (Figure 2). Warming is greater over the northern hemisphere (NH) than the southern hemisphere (SH) over all time periods, and the magnitude of warming is strongest over all regions in the CCSM4 prior compared to that in the LMR. Over both the CCSM4 prior and the LMR, there is warming over the Arctic, though the location of maximum warming is different: in the CCSM4 prior, warming is greatest over the Greenland-Iceland-Norwegian (GIN) seas, while warming is greatest in the LMR over the Barents sea. In the LMR, variability is relatively stationary over all time periods, though differences in warming over the high northern latitudes are apparent; in the pre-industrial period (pre-1850), warming over northern Eurasia is most prominent, while warming over boreal North America and central Asia dominates in the industrial period.

Comparison of the 20-year low-pass filtered regression of the AMO index on temperature (Figure 2a to d) with the unfiltered regression (Figure 2e to h) reveals that the temperature response associated with AMV is stronger at the shorter time scales that dominate the unfiltered regression.

Over all time periods in the LMR (years 0 to 1850, years 1200 to 1850, and years 1850 to 2000), warming is not uniform over the north Atlantic basin: maxima in warming are evident at 50N and 5N (Figure 3a to d). Over shorter timescales than those explored in the remainder of this study, however, the two-lobed pattern becomes a horseshoe with the tropical and midlatitude warming maxima linked by warming over the eastern Atlantic (compare Figure 3a-d to Figure 3e-h). This distinct horseshoe pattern of warming over the midlatitudes and tropics that characterizes north Atlantic SSTs variability at shorter time scales has been noted by others, and is the leading mode of variability found with empirical orthogonal functional decomposition

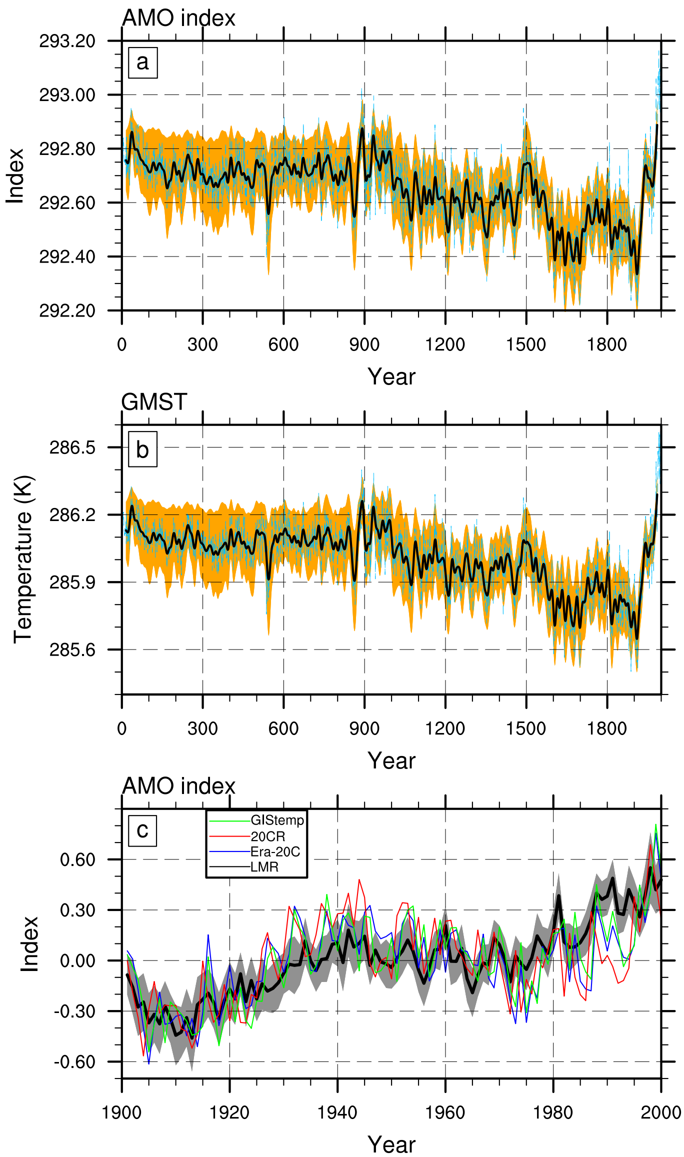

Figure 1. (a) Atlantic Multidecadal Oscillation (AMO) index time series and (b) global mean surface temperature (GMST) time series computed from the LMR over the last 2000 yrs, with the yearly time series (light blue, dotted) and 20-year low-pass time series (black; 95% confidence interval shown in orange); and (c) AMO index over the last 100 yrs (bottom) as computed from the LMR (black; 95% confidence interval shown in grey), the 20th Century Reanalysis (20CR, red), the ERA-20C reanalysis (Era-20C, blue), and the NASA GIStemp reanalysis (GIStemp).

Clim. Past Discuss., doi:10.5194/cp-2017-49, 2017
Manuscript under review for journal Clim. Past
Discussion started: 15 May 2017

Climate of the Past Discussions
Open Access

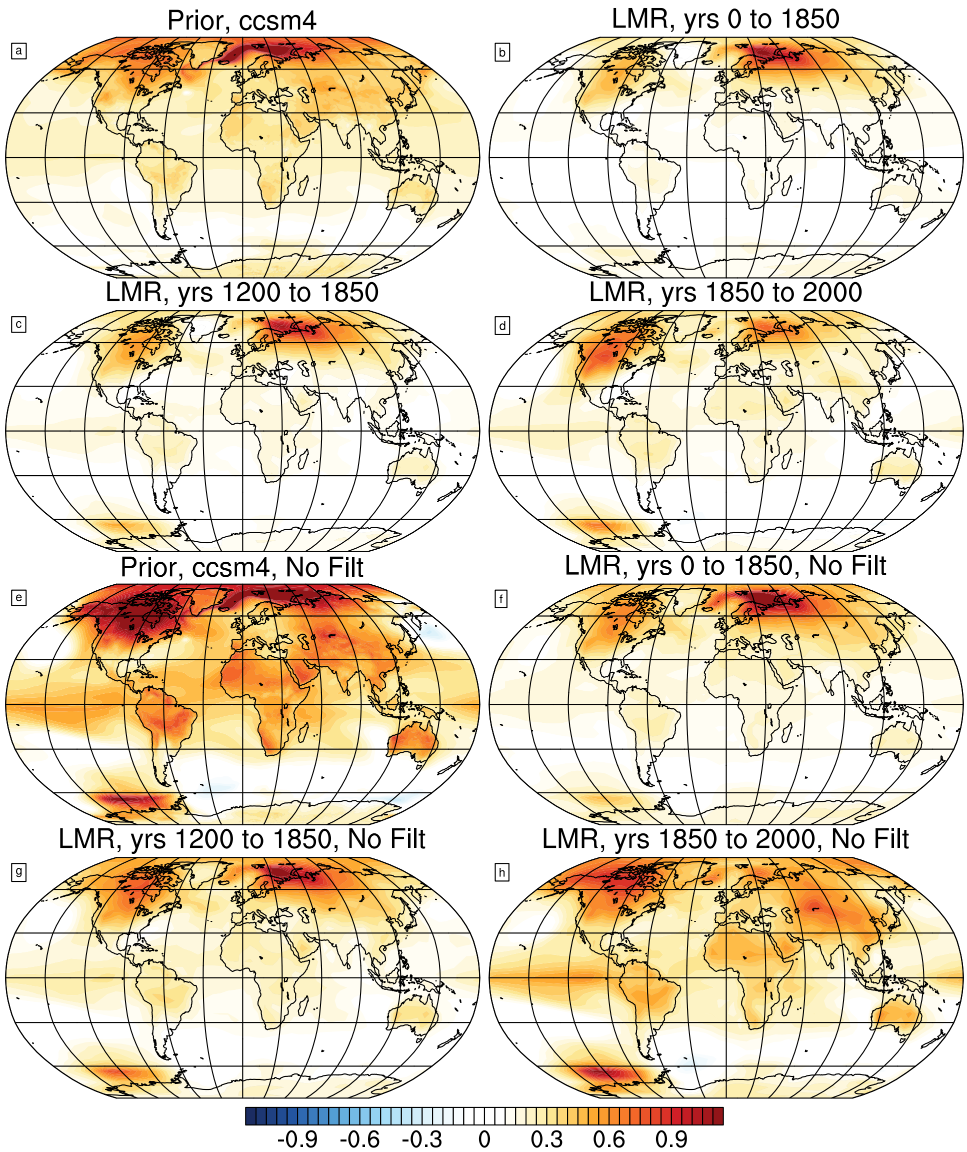

Figure 2. Low-pass filtered regression of the AMO index on surface temperature (in K) in (a) the CCSM4 prior; (b) the LMR from years 0 to 1850; (c) the LMR from years 1200 to 1850; and (d) the LMR from years 1850 to 2000. Panels (e) through (h) are similar as (a) through (d), but show the unfiltered regression.

Clim. Past Discuss., doi:10.5194/cp-2017-49, 2017
Manuscript under review for journal Clim. Past
Discussion started: 15 May 2017

Climate of the Past
Discussions

analysis over this region (see, e.g., Hartmann, 1994). Because our focus is on longer timescale variability, we will utilize 20-year low-pass filtering for the rest of our analysis (except for time-series analysis of the AMV, §3.4).

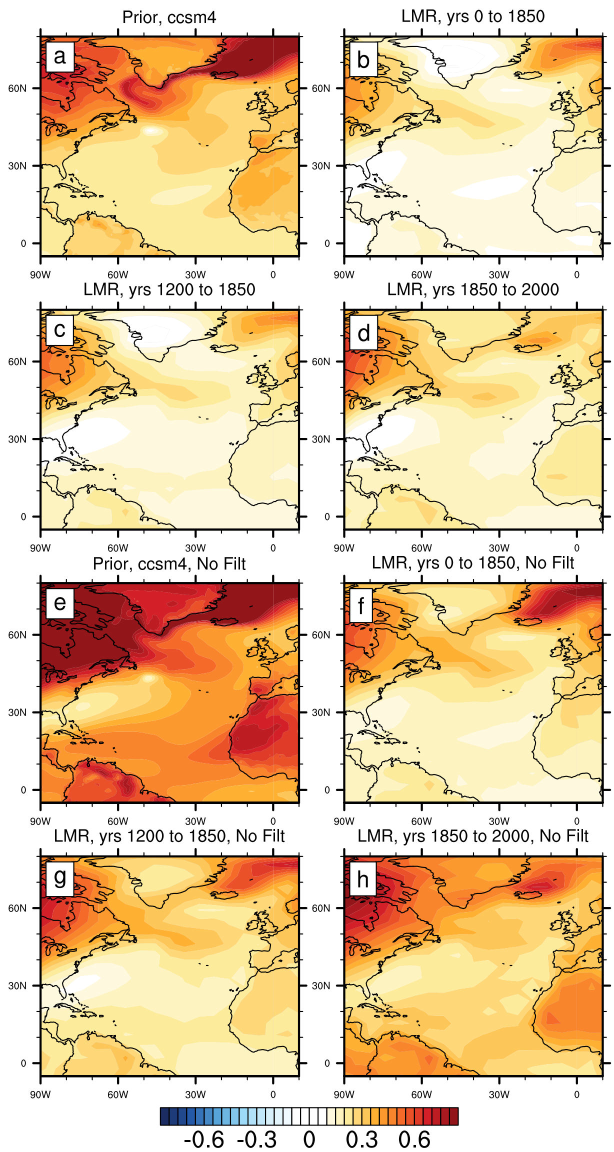

Figure 3. As in Figure 2, over the north Atlantic basin.

During the positive phase of the AMO, the LMR shows that warming over the high latitude north Atlantic is linked to retreat of sea ice from the GIN and Barents seas (Figure 4, contours), with strong spatial agreement between the LMR over all time periods. In contrast, the CCSM4 prior shows a much more sharply-defined spatial pattern of sea ice retreat than the LMR, though the general regions of retreat are the same. Sea ice also thins over much of the Arctic (Figure 4, colors) in both the

Clim. Past Discuss., doi:10.5194/cp-2017-49, 2017
Manuscript under review for journal Clim. Past
Discussion started: 15 May 2017

Climate of the Past Discussions
Open Access
EGU

LMR and CCSM4 prior; in the CCSM4, sea ice thins over the entire Arctic, while in the LMR, there is a small region of sea ice thickening centered about the Beaufort Sea. This thickening of ice in the Beaufort sea is linked to a low pressure center over the Arctic in the LMR, which is not present in the CCSM4 prior (or in other reanalyses of the instrumental period). Sea ice retreat coincident with the positive phase of the AMO has also been shown in model-based studies (see, e.g. Miles et al., 2014). Such retreat and thinning of sea ice is also consistent with increased ocean heat transport into the north Atlantic, possibly due to strengthening of the AMOC during the positive phase of the AMO (considered further in §3.3).

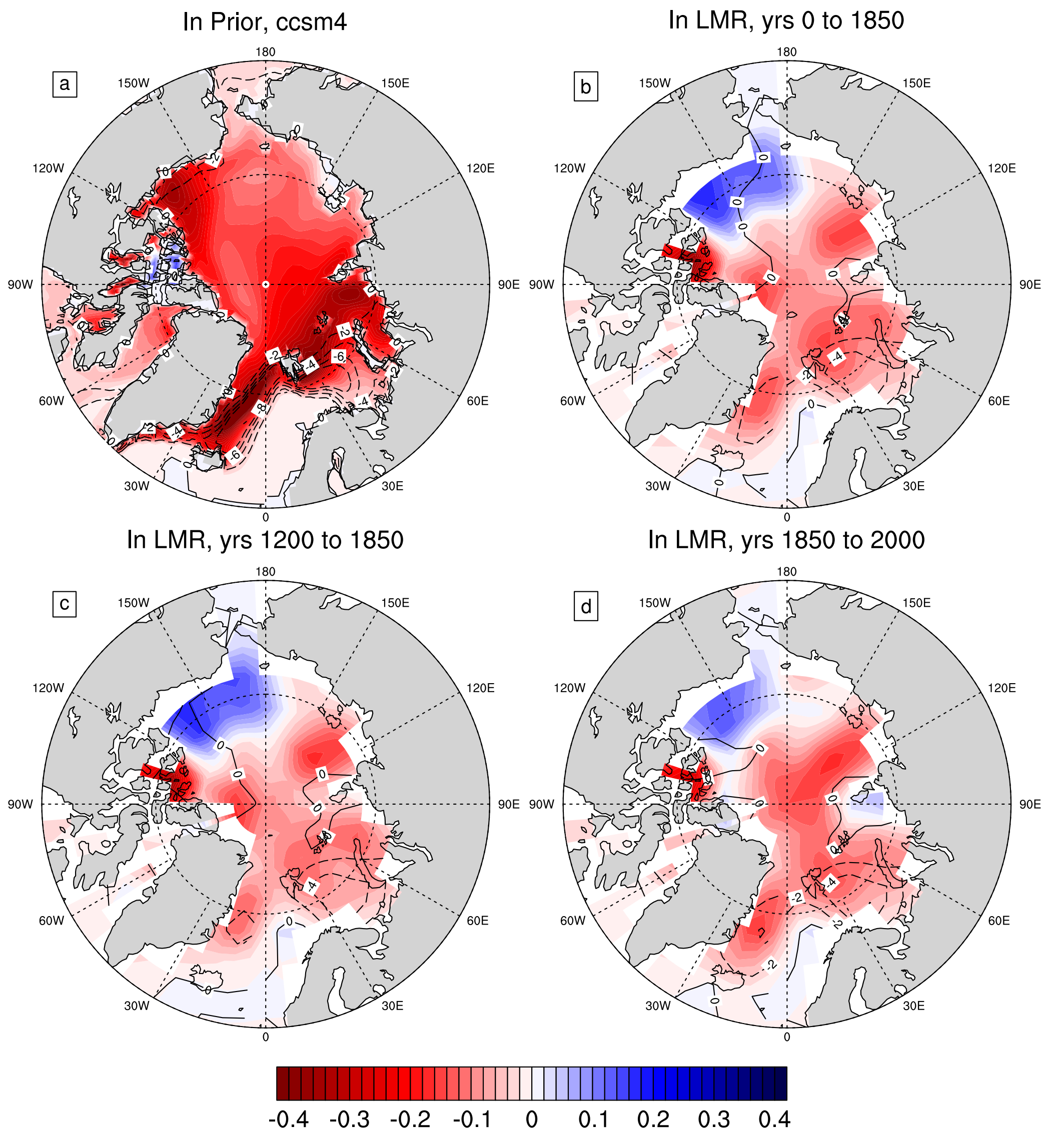

Figure 4. As for Figure 2, panels (a) to (d), but for the low-pass filtered regression of the AMO index on sea ice thickness (colors, in m) and on sea ice concentration (contours, %).

Clim. Past Discuss., doi:10.5194/cp-2017-49, 2017
Manuscript under review for journal Clim. Past
Discussion started: 15 May 2017

Climate of the Past Discussions

While warming associated with AMV is strongest over the high northern latitudes, associated precipitation changes are most prominent at the equator over all basins (Figure 5). Surprisingly, the magnitude of these changes is larger in the LMR (1200 to 1850 and 1850 to 2000) than in the CCSM4 prior, though temperature increases associated with AMV are largest in the latter (recall Figure 2). On the other hand, the magnitude of these changes is very small over yrs 0 to 1850 CE in the LMR, possibly due to poor proxy coverage during the earlier part of this period. Most changes in precipitation are co-located in the CCSM4 prior and the LMR, though the LMR predicts stronger AMV-linked drying over the Maritime continent than found in the CCSM4 prior. In general, the magnitude of the increase in precipitation is greatest in the NH, and a northward shift in the equatorial precipitation maximum (the Intertropical Convergence Zone, i.e. ITCZ) is particularly evident over the Atlantic basin (see also Knight et al., 2006). We also note that the double ITCZ apparent in the CCSM4 prior is consolidated into a single precipitation maximum in the LMR.

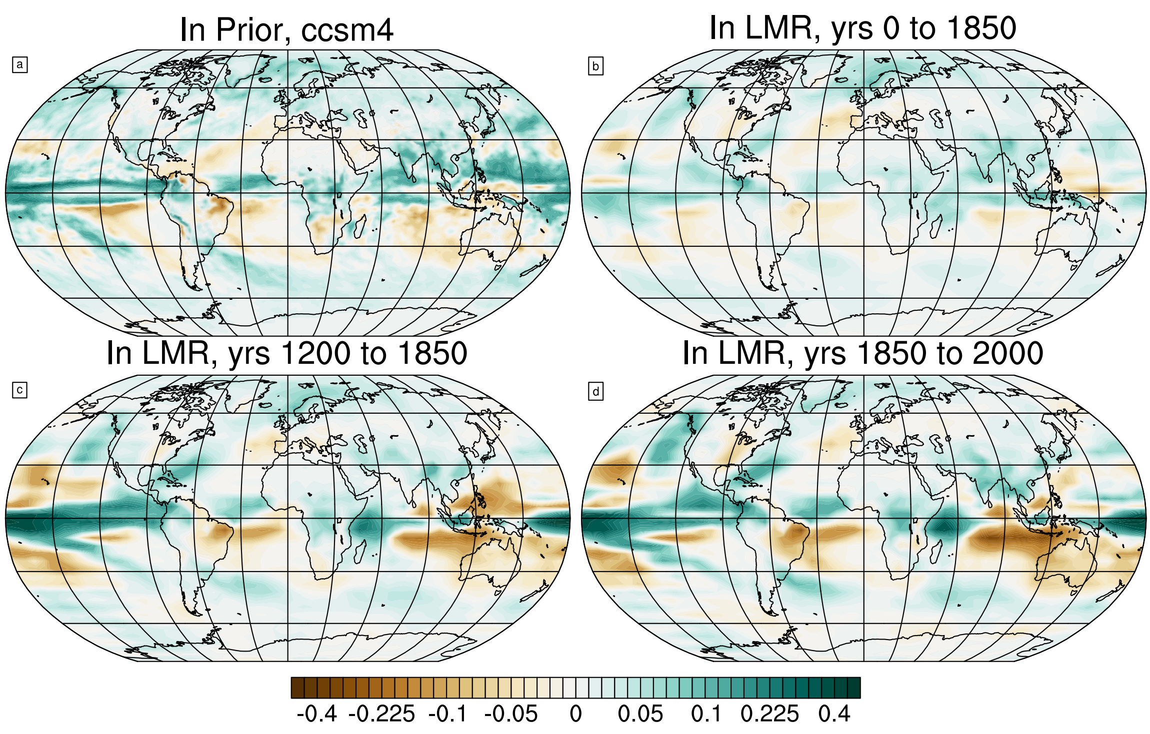

Figure 5. As for Figure 2, panels (a) to (d), but for the low-pass filtered regression of the AMO index on precipitation (in mm/day).

3.3 Energetics

The energetics associated with a positive AMO index differ significantly between the LMR and the CCSM4 prior. While surface and TOA fluxes and their imbalances are qualitatively similar between the LMR and the CCSM4 prior, we find that the energy transports implied by these fluxes differ between the LMR and CCSM4 prior. Overall, the energetics and implied

Clim. Past Discuss., doi:10.5194/cp-2017-49, 2017
Manuscript under review for journal Clim. Past
Discussion started: 15 May 2017

dynamics in both the LMR and CCSM4 prior are consistent with most findings from previous studies (see, i.e. Knight et al., 2006), though there are some discrepancies. We describe these findings in detail below.

In the LMR, a positive AMO index is linked to net top-of-atmosphere (TOA) radiative flux (positive upward) anomalies that are negative in the NH and positive in the SH over all time periods (Figure 6a). While the anomaly in the TOA incoming shortwave (SW) flux is nearly zero (Figure 6b), large compensating changes in the outgoing SW flux and outgoing longwave (LW) flux mostly determine the net TOA radiative flux (Figures 6c and d, respectively). The outgoing SW flux anomaly is negative nearly everywhere (i.e. the outgoing SW flux decreases), with the LMR showing the strongest anomalies north of the equator. These anomalies are consistent with either an increase in atmospheric SW absorption by water vapor in the warmer hemisphere or a decrease in reflected SW due to fewer clouds in the warmer hemisphere. The outgoing LW flux increases nearly globally, commensurate with increased temperatures at the effective radiating level associated with warming during the positive phase of the AMO. This increase in outgoing LW radiation dominates in the SH, while the decrease in outgoing SW radiation dominates in the NH, implying a net southward meridional energy transport in the LMR (see Figure 8a and accompanying text). At the equator, there is an increase in the outgoing SW radiation, which is balanced by a decrease in the outgoing LW radiation; both are consistent with greater cloudiness in the deep tropics and strengthening of the equatorial precipitation noted earlier (Figure 5).

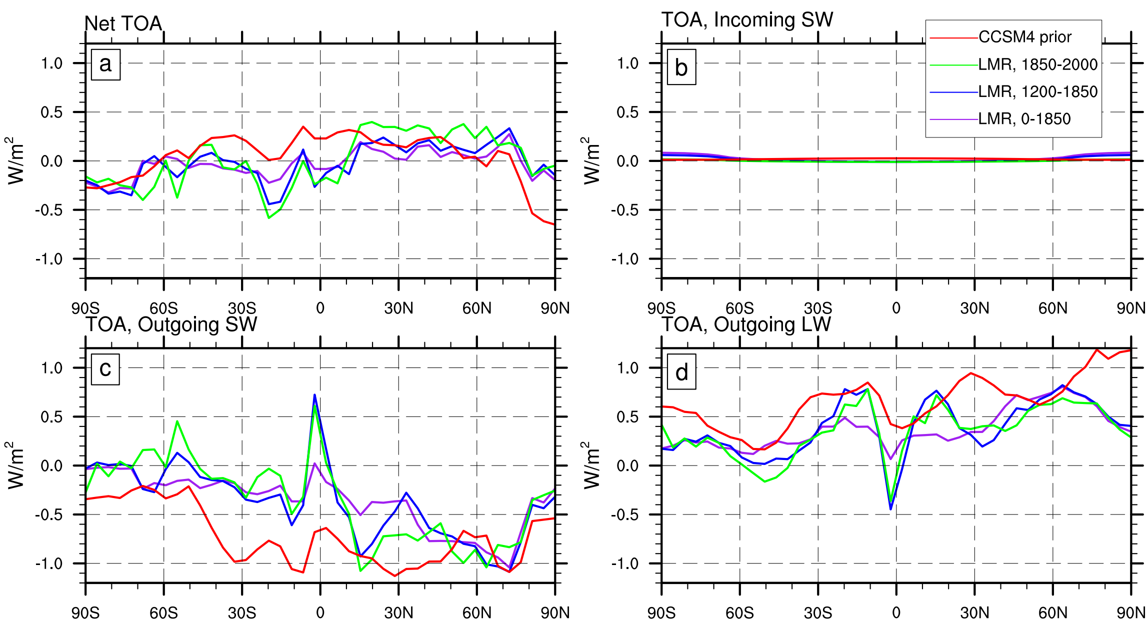

Figure 6. Low-pass filtered regression of the AMO index on top-of-atmosphere (TOA) energy fluxes (in W/m^2) in the LMR (from years 0 to 1850, 1200 to 1850, and 1850 to 2000) and the CCSM4 prior: (a) net (incoming) flux, (b) incoming shortwave (SW) flux, (c) outgoing SW flux, and (d) outgoing longwave (LW) flux.

In the CCSM4 prior, the TOA radiative fluxes suggest a very different picture. While the outgoing SW flux decreases (Figure 6c) and the outgoing LW flux increases (Figure 6d) as in the LMR, the sum of these, the net upward TOA flux (Figure 6a), is positive in the high latitudes in both hemispheres and negative in the lower and mid- latitudes; as a result, the implied meridional total energy transport in the CCSM4 prior is polewards in both hemisphere.

At the surface, both the LMR and the CCSM4 prior have net fluxes associated with a positive AMO index that are downwards in the tropics, upwards in the subtropics and midlatitudes, and downwards in the NH high latitudes (Figure 7a). This pattern is most pronounced in the CCSM4 prior, but is also evident over all time periods in the LMR. Globally, we find that this spatial pattern results from decreases in both the net (upward) surface SW radiation (i.e. an increase in SW coming down at the surface; Figure 7b) and the net (upward) surface LW radiation (i.e. an increase in the LW coming down at the surface; Figure 7c); these increased surface SW and LW radiative fluxes are mostly balanced by an increase in the surface latent heat flux (Figure 7e), which renders the net surface flux small over most latitudes. At the equator, an increase in the net (upward) surface SW radiation and a decrease in the net (upward) surface LW radiation is consistent with greater cloud cover. Sensible heat flux anomalies at the surface are small everywhere (Figure 7d).

These results from the LMR suggest that the positive phase of the AMO is associated with greater atmospheric water vapor, likely a result of Clausius-Clapeyron scaling of atmospheric moisture with temperature. These findings, together with the TOA fluxes described earlier, also suggest that the positive phase of the AMO is associated with fewer (reflective) low clouds in the extra-tropics and more clouds near the equator; the latter is in agreement with positive precipitation anomalies in the deep tropics (recall Figure 5).

As alluded to earlier, differences in the net TOA radiative fluxes between the LMR and the CCSM4 prior imply very different total energy transport anomalies. The total implied meridional energy transport, TET, at latitude ϕ_0 can be computed using the zonally-averaged net TOA fluxes $R_{TOA}(\phi)$ as

$$TET(\phi_0) = r_{earth}^2 \int_0^{2\pi} \int_0^{\phi_0} (R_{TOA}(\phi) - R_{storage}(\phi)) \cos(\phi) d\phi d\theta \tag{4}$$

where ϕ and θ are the latitude and longitude coordinates, respectively, r_{earth} is the radius of Earth, and $R_{storage}(\phi)$ is the heat storage tendency of the climate system at latitude ϕ (Peixoto and Oort, 1992). We find that the TET is anomalously southward north of 20S and northward south of 20S for the LMR over later time periods (1200 to 1850 and 1850 to 2000), and is particularly large between 10S and 20N (Figure 8a). In the CCSM4 prior, on the other hand, the TET is anomalously southward south of 10N and anomalously northward north of 10N.

The atmospheric energy transport, AET, at latitude ϕ_0 is computed using the difference between $R_{TOA}(\phi)$ and net surface flux $R_{Sfc}(\phi)$ as

$$AET(\phi_0) = r_{earth}^2 \int_0^{2\pi} \int_0^{\phi_0} (R_{TOA}(\phi) - R_{Sfc}(\phi)) \cos(\phi) d\phi d\theta \, . \tag{5}$$

The AET anomaly associated with a positive AMO is southwards at most latitudes in both the LMR (over all time periods) and in the CCSM4 prior (Figure 8b). The maximum southward AET is further northward in the LMR compared to the CCSM4

Clim. Past Discuss., doi:10.5194/cp-2017-49, 2017
Manuscript under review for journal Clim. Past
Discussion started: 15 May 2017

Climate of the Past
Discussions
Open Access
EGU

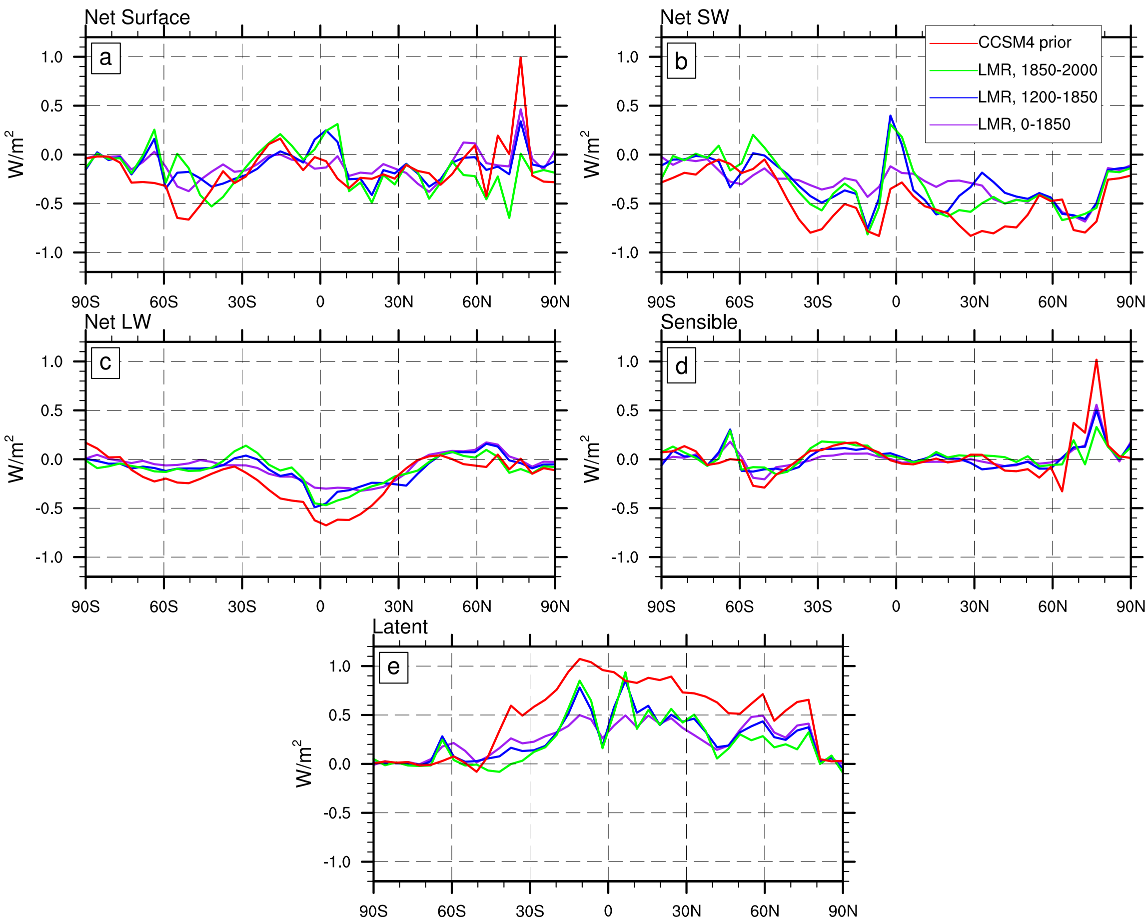

Figure 7. Low-pass filtered regression of the AMO index on surface energy fluxes (in W/m^2) in the LMR (from years 0 to 1850, 1200 to 1850, and 1850 to 2000) and the CCSM4 prior: (a) net (downward) surface flux, (b) net (upward) SW flux, (c) net (upward) LW flux, (d) sensible heat flux, and (e) latent heat flux.

prior (close to the equator in the former, while in the southern midlatitudes in the latter). The increase in southward cross-equatorial energy transport in the LMR is consistent with the northward shift of the ITCZ noted previously (recall Figure 5). The increase in southward cross-equatorial energy transport is also consistent with an increase in the inter-hemispheric temperature difference associated with the AMO which preferentially warms the NH over the SH (recall Figure 2; also see Friedman et al., 2013), which arises from a strengthening of the Hadley circulation in the cooler hemisphere. On the other hand, the increase seen in the CCSM4 prior occurs most prominently in the midlatitudes, suggesting a strengthening of poleward energy transport by midlatitude eddies in the SH rather than an adjustment of the tropical circulation.

The oceanic energy transport $OET(\phi_0)$ is computed as a residual from the TET and AET:

$$OET(\phi_0) = TET(\phi_0) - AET(\phi_0)\ . \tag{6}$$

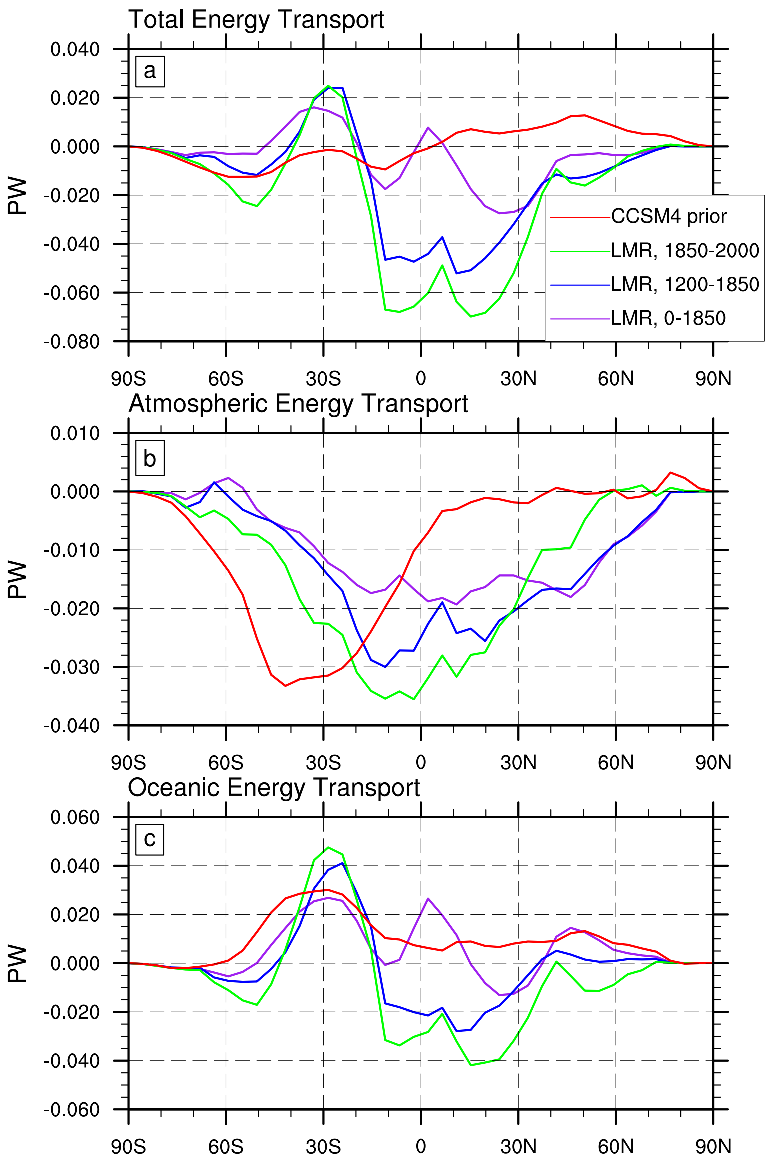

Figure 8. Low-pass filtered regression of the AMO index on energy transport (in PW) in the LMR: (a) total energy transport, (b) atmospheric energy transport, and (c) oceanic energy transport for the LMR from years 0 to 1850 (purple lines), LMR from years 1200 to 1850 (blue lines), LMR from years 1850 to 2000 (green lines), and CCSM4 prior (red).

From Figure 8c, it is clear that, aside from the subtropical SH, the LMR and CCSM4 prior differ significantly in anomalous OET associated with the positive phase of the AMO. In the LMR (over 1200 to 1850 and 1850 to 2000), energy transport by the ocean is anomalously southward in the NH and northward in the SH, with a significant southward cross-equatorial component; much of the anomalous transport is confined to the subtropics. These anomalies are larger over the 1850-2000 time period, and are consistent with a decrease in oceanic energy transport by the wind-driven subtropical gyres and subtropical cells when the AMO is in its positive phase. A large southward cross-equatorial component to the OET anomaly suggests a decrease in northward cross-equatorial energy transport by the AMOC. In the CCSM4 prior, on the other hand, the OET response is anomalously positive at all latitudes, suggesting that an increase in northward energy transport by the AMOC corresponds to a positive AMO index.

In both the LMR and CCSM4 prior, we find that the average net TOA flux over the last 2000 years is positive, indicating that energy is being removed from the Earth system; when the AMO index is positive, however, the net TOA flux decreases such that energy is being anomalously added to the Earth system relative to the mean state (Table 2). The extent to which this occurs is similar between the CCSM4 prior and the LMR over all time periods, suggesting that this aspect of AMV has been stationary over the last 2000 years.

Net TOA Imbalance (W/m^2)	Global Mean	Regressed on the AMO Index
LMR, 0-1850	0.46	0.01
LMR, 1200-1850	0.31	-0.01
LMR, 1850-2000	0.37	0.01
CCSM4 prior	0.61	0.19

Table 2. Net top-of-atmosphere (TOA) flux imbalances in the LMR (from years 0-1850, 1200-1850, and 1850-2000) and the CCSM4 prior, shown for the global mean and regressed on the AMO index. Fluxes out of the Earth system (i.e. upward) are positive.

Surface flux imbalances in the LMR (Table 3) are also qualitatively similar to the TOA flux imbalances, with positive surface flux anomalies characterizing the mean state over all time periods (i.e. energy is leaving the oceans), consistent with millennial-scale cooling. When the AMO is in its positive phase, on the other hand, the surface flux anomaly decreases, indicating that energy is being anomalously absorbed by the oceans relative to the mean state. This is consistent with the TOA flux imbalance linked to a positive AMO index, which also decreases relative to the mean. The results from the CCSM4, however, are more energetically consistent in the magnitude of the energy uptake by the climate system when the AMO is in its positive phase (0.19 W/m^2 and 0.18 W/m^2 for the TOA and surface flux imbalances, respectively) compared to the LMR (e.g. 0.01 W/m^2 and 0.13 W/m^2 for the TOA and surface flux imbalances, respectively, in the LMR over the years 0 to 1850 CE).

3.4 Time Scales of Variability

We now consider what time scales characterize AMV. Tung and Zhou (2013) show a distinct 50- to 80-year peak in the Central England Temperature record (HadCET; see Parker et al., 1992), and suggest that this variability may be related to coherent

Clim. Past Discuss., doi:10.5194/cp-2017-49, 2017
Manuscript under review for journal Clim. Past
Discussion started: 15 May 2017

Net Surface Imbalance (W/m^2)	Global Mean	Regressed on the AMO Index
LMR, 0-1850	1.79	0.13
LMR, 1200-1850	1.81	0.12
LMR, 1850-2000	1.76	0.14
CCSM4 prior	1.91	0.18

Table 3. Net surface flux imbalances in the LMR (from years 0-1850, 1200-1850, and 1850-2000) and the CCSM4 prior, shown for the global mean and regressed on the AMO index. Fluxes out of the surface (i.e. upward) are positive.

variability in north Atlantic SSTs. Other studies have synthesized proxy records from the north Atlantic basin over the last 500 years to infer the existence of such a multidecadal oscillation over the last millennium (see, i.e. Delworth and Mann, 2000; Gray et al., 2004). Furthermore, Knudsen et al. (2011) suggest that multidecadal variability, non-stationary and possibly linked to north Atlantic SSTs, is evident in global ice core and sedimentary records over a span of the last 8,000 years.

Motivated by previous research, we now analyze what AMV time scales are evident in the LMR reconstruction of north Atlantic SSTs. The LMR uses records from proxies over the last two millennia, weighted heterogeneously relative to the prior, and includes the proxy data used by Delworth and Mann (2000), Gray et al. (2004), and others; these records are processed here using the data assimilation algorithm described herein (see Methods, §2; also Hakim et al., 2016). If time scales present in individual proxy record time series are indicative of variability over the large-scale north Atlantic in general, these time scales should also be present in the reconstructed AMO index.

Wavelet analysis of the AMO index is performed on six different LMR reconstructions that use three distinct calibration datasets (MLOST, GIS, and CRU; see Table 1) and two different model priors (CCSM4 and MPI; see Table 1). The reconstructions reveal statistically significant power over different time periods at several different time scales, and the details vary with the reconstruction (Figure 9). For all reconstructions, longer time scale variability (> 40 years) is only evident over the latter portion of the record (mostly after year 800 CE). The MLOST-MPI reconstruction, in particular, shows very little of this longer time scale variability, while the CRU-CCSM4 reconstruction displays it prominently. None of the reconstructions show longer time scale variability in the early portion of the record, though several of the reconstructions reveal an event at year 500; this may reflect either a lack of proxy records over this period or non-stationarity in the climate system over the preindustrial period.

We assess the significance of variability at these different time scales using the global wavelet power spectrum, which is an average of the coincident wavelet power at each time scale over the entire record. These global power spectra, shown in Figure 10a, suggest that there is no distinct multidecadal spectral peak in the AMV. Many of the reconstructions suggest reddening of the spectrum near the 50-to-60-year time scale, particularly those reconstructions using the GIS and MLOST calibration datasets, though none of these are statistically significant at $p < 0.05$. Furthermore, reconstructions using the CRU calibration dataset show that longer time scale (≥ 90 year) variability cannot be explained by a simple AR(1) process. However, our results appear to rule out the presence of distinct multidecadal oscillations in north Atlantic SSTs over the last two millennia. We find

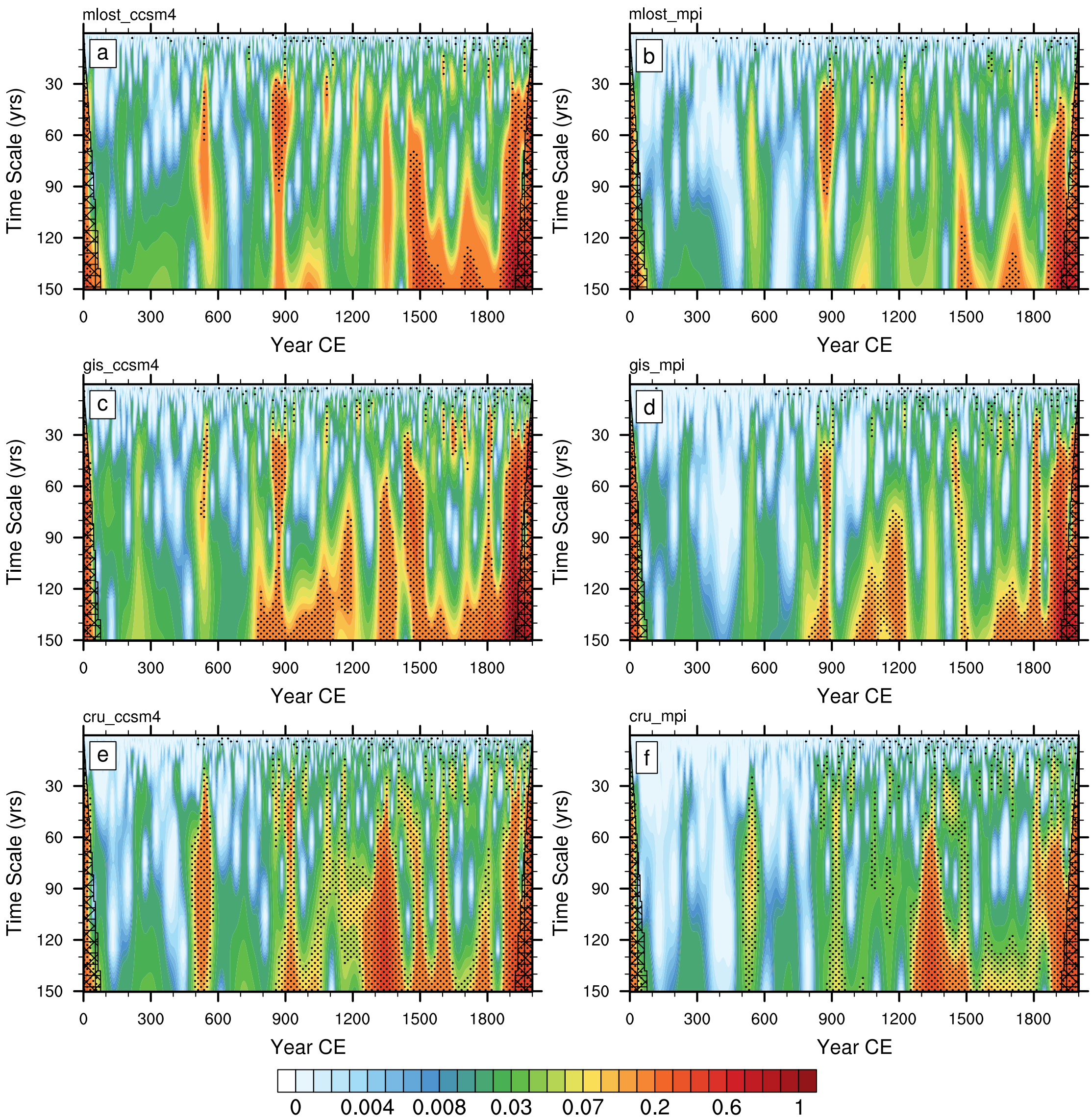

Figure 9. Wavelet analysis of AMO time series from 6 different LMR reconstructions: (a) MLOST-CCSM4, (b) MLOST-MPI, (c) GISTEMP-CCSM4, (d) GISTEMP-MPI, (e) CRU-CCSM4, and (f) CRU-MPI. All analyses are performed using the Paul wavelet. Stippled areas are statistically significant at $p < 0.05$, and the hatched region demarcates the cone of influence.

Clim. Past Discuss., doi:10.5194/cp-2017-49, 2017
Manuscript under review for journal Clim. Past
Discussion started: 15 May 2017

that this result is insensitive to the wavelet type and is not affected if a shorter time period is used for the analysis (e.g. years 1200 to 2000 CE). Furthermore, we find that the global power spectrum is very quantitatively similar when the same analysis is performed using a fixed-proxy network for the reconstruction (i.e. one in which all proxy records are continuous for the entire time period of the analysis), further suggesting that these results are insensitive to the choice of proxy network used. In addition, multitaper spectra (Thomson, 1982) confirm that none of our AMO reconstructions exhibit any spectral power at multidecadal time scales above that expected from red noise (not shown), consistent with results gleaned from the global wavelet power spectrum (Figure 10a).

While we do not find a statistically significant multidecadal spectral peak in AMV, we do find a significant 3-to-4-year spectral peak (Figure 10b). We suggest that this peak may be a result of teleconnections with the tropical Pacific and El Nino - Southern Oscillation (ENSO) variability therein, which has a similar time scale (see, e.g Dong et al., 2006). We reserve study of connections between tropical Pacific and Atlantic variability for future work.

3.5 Limitations of LMR Investigation of AMV and other variability

While we have been able to show that the LMR captures thermodynamic aspects of the AMO, there are factors that limit its utility in investigating the dynamics of the AMO. While proxy records synthesize information about temperature and precipitation, their utility for reconstructing fields that are relatively invariant to temperature remains uncertain. We find that dynamic spatial fields like surface pressure and winds are not well-reconstructed by the LMR (not shown); therefore, we have not included such reconstructions in this analysis. The limitations of paleoclimate reanalyses using proxies that record primarily thermodynamic variables, rather than dynamic ones, remains an open question, which will be considered in future work.

4 Discussion

We have considered the thermodynamics of AMV over the last 2000 years using the LMR, a paleoclimate reanalysis method that objectively assimilates information from paleoclimate records. Several aspects of our findings regarding AMV agree with previous model-based and observational studies of north Atlantic SST evolution. We find that a positive AMO index coincides with warmer continents, a two-lobed pattern of warming over the Atlantic, and a warmer Arctic (Kushnir, 1994; Delworth and Mann, 2000; Chylek et al., 2009). In the Arctic, sea ice retreats from the Greenland-Iceland-Nordic seas and thins over much of the Arctic Ocean (Miles et al., 2014). Globally, precipitation increases and the ITCZ strengthens and shifts northward (Knight et al., 2006).

With the LMR, we also find several elements of AMV that have not been reported in the literature. When the AMO is in its positive phase, southward cross-equatorial energy transport increases, mostly mediated by the atmosphere (the northward shift in the equatorial precipitation); these latter changes are consistent with energy balance requirements as necessitated by stronger warming in the NH than the SH during the positive phase of the AMO, i.e. an effect of the increase in the interhemispheric temperature anomaly (see Friedman et al., 2013). The LMR also shows that when the AMO is in its positive phase, the

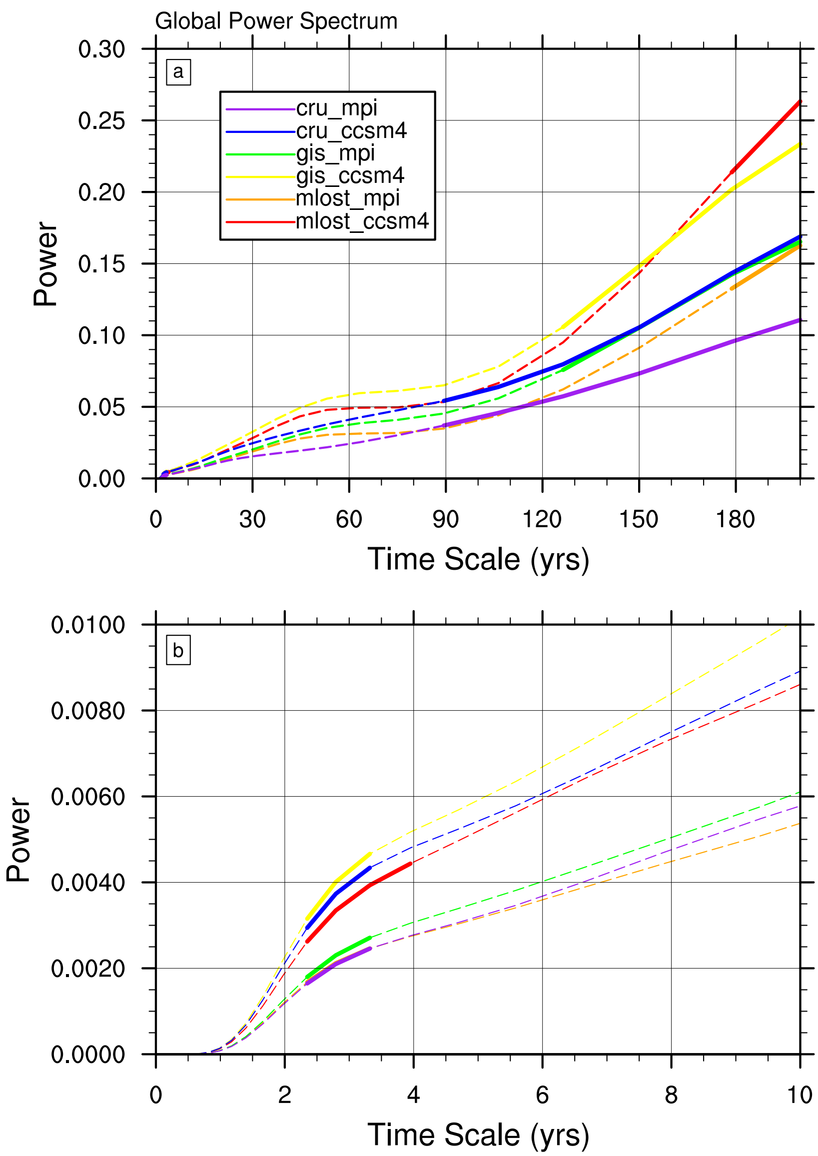

Figure 10. Global wavelet spectra of reconstructions shown in Figure 9 (a) for time scales between 0 to 200 years, and (b) zoomed in to show time scales between 2 and 10 years. Time scales that are statistically significant over the red noise background (at $p < 0.05$) are shown as solid lines, while time scales that are not statistically significant are shown as dotted lines.

Earth system loses less (net) energy to space, with much of this excess energy absorbed by the oceans. TOA and surface flux anomalies are consistent with an increase in atmospheric specific humidity and a decrease in low (reflective) clouds.

Our study of the AMV using the LMR demonstrates that climate field reconstruction methods, which assimilate information from the proxy record, can provide valuable information on climate variability in the Earth system. While correlations between north Atlantic SSTs and various thermodynamic fields (temperature, precipitation, and sea ice) are similar in the LMR and the CCSM4 prior, the LMR provides a temporal reconstruction of the AMO index that informs our understanding of AMV beyond that from the model prior. First, energetic changes associated with AMV are distinct in the LMR and CCSM4 prior, with the LMR predicting consistent changes in the cross-equatorial energy transport, tropical circulation, and extratropical cloud cover that are not found in the CCSM4 prior. Second, the LMR helps resolve the dominant time scales that characterize AMV. Since there is little agreement between various GCMs regarding the dominant time scales that characterize AMV (see Clement et al., 2015), LMR reconstruction of the AMO index is invaluable. Our results suggest that the proxy observations over the last 2000 years, when objectively assimilated, do not exhibit a multidecadal timescale.

The lack of a distinct multidecadal spectral peak in the LMR reconstruction of the AMO is in contrast to other studies that have found such variability in individual observational records (see, e.g. Tung and Zhou, 2013) or limited collections of proxies (see, e.g. Delworth and Mann, 2000; Gray et al., 2004). We point out that such a significant spectral peak in an individual record or collection of records does not necessarily translate into a coherent mode of basin-scale multidecadal variability. While certain records may display oscillations, a basin-scale oscillation requires both spatial coherence and matching time scales in these records over certain regions. The objective assimilation procedure used in the LMR climate field reconstruction utilizes the information provided by the proxy records investigated in these previous studies; the results of this objective assimilation suggest that there is no distinct multidecadal or centennial spectral peak in AMV, though there is reddening of the spectra. These results support the null hypothesis presented by Clement et al. (2015), and suggest that there may be little need to consider longer time scale processes when studying the mechanism of AMV over the late Holocene, particularly the preindustrial period.

In our reconstructions, multidecadal spectral power is evident only over the latter portion of the LMR, year 1500 CE forward, and is particularly pronounced following year 1900 CE. While there has been much hypothesized regarding these oscillations in the instrumental record, and whether they are a result of internal climate variability or a result of external forcing (see, e.g. Booth et al., 2012; Zhang et al., 2013, and others), we point out two important characteristics of the instrumental period that render it a poor era for studying multidecadal variability in the climate system. First, the instrumental record is very short; as a result, there is very little that can be said about multidecadal time scale variability over this time period that carries any statistical weight (see, e.g., Wunsch, 1999; Vincze and Janosi, 2011). Second, the instrumental period is one in which the climate system has been strongly anthropogenically forced, suggesting that any variability observed over this period may differ significantly from variability from the preindustrial era when anthropogenic forcing was much smaller. Indeed, Tandon and Kushner (2015) show that in models, the lead-lag relationship between north Atlantic SSTs and the AMOC are very different between the preindustrial and modern periods, suggesting a shift in the mechanism underlying AMV between these two time periods. Both of these limitations suggest that caution must be exercised in extrapolating characteristics of multidecadal variability in the Earth system from the instrumental record.

We also point out that our objective data assimilation approach cannot completely rule out a distinct multidecadal spectral peak in north Atlantic SSTs. While we have shown that objective data assimilation of the proxy record to reconstruct the surface temperature field over the last two millennia does not yield any evidence of multidecadal variability, it is likely that further improvements in the proxy network, the proxy system models, or the data assimilation procedure will improve the reconstruction in such a way as to modify our current conclusions. From this study, however, we can say that the surface temperatures reconstructed over the last 2000 years, which are obtained from assimilating the existing network of proxies using today's state-of-the-art methods, do not provide compelling evidence for multidecadal variability over the north Atlantic.

We conclude by pointing out some important limitations of studies of climate variability using the LMR. First, the data assimilation approach itself is Gaussian, which may limit its utility in regimes very different from that of the base climate state. Second, LMR reconstructions depend on the climate models, proxies, and observation models that are used to create them. These components, in turn, are being continually tuned and refined. Third, it is unknown what effects the limitations in the size and distribution of the proxy network have on the reconstruction made possible by the LMR. In particular, we note that the more limited network from the early portion of the instrumental record (pre-1200 CE) may affect the reconstruction and its variability. Further study will be required to assess sensitivity to the sparsity of the proxy network. Finally, we note that there are other ways to improve paleoclimate reanalyses using proxy records, including the incorporation of linear inverse modeling into the reconstruction methodology to achieve on-line data assimilation (see Perkins and Hakim, 2016). In the future, such refinement of reconstruction methods will help to further study of the Earth system over its long and varied climatic history.

5 Code availability

The data assimilation software for the LMR project will be publicly released at the end of the project in 2018.

Competing interests. None.

Disclaimer. None.

Acknowledgements. HKAS thanks Andre Perkins for informative discussions and technical help. All authors acknowledge funding support from the following sponsors to the University of Washington: National Science Foundation (award AGS-1304263 and AGS-1602223) and National Oceanic and Atmospheric Administration (award NA14OAR4310176). All authors also acknowledge the World Climate Research Program's Working Group on Coupled Modeling, which is responsible for CMIP, and thank the climate modeling groups (CCSM4 and MPI, listed in Table 1) for producing and making available their model output. For CMIP the U.S. Department of Energy's Program for Climate Model Diagnosis and Intercomparison provides coordinating support and led development of software infrastructure in partnership with the Global Organization for Earth System Science Portals.

Clim. Past Discuss., doi:10.5194/cp-2017-49, 2017
Manuscript under review for journal Clim. Past
Discussion started: 15 May 2017

Climate of the Past
Discussions

References

Booth, B., Dunstone, N., Halloran, P., Andrews, T., and Bellouin, N.: Aerosol implicated as a prime driver of twentieth-century North American climate variability, Nature, 484, 228–232, 2012.

Chylek, P., Folland, C., Lesins, G., Dubey, M., and Wang, M.: Arctic air temperature change amplification and the Atlantic Multidecadal Oscillation, Geophysical Research Letters, 36, 2009.

Chylek, P., Folland, C., Dijkstra, H., Lesins, G., and Dubey, M.: Ice-core data evidence for a prominent near 20 year time-scale of the Atlantic Multidecadal Oscillation, Geophysical Research Letters, 38, 2011.

Clement, A., Bellomo, K., Murphy, L., Cane, M., Mauritsen, T., Radel, G., and Stevens, B.: The Atlantic Multidecadal Oscillation without a role for ocean circulation, Science, 350, 320–324, 2015.

Consortium, P.: Continental-scale temperature variability during the past two millennia, Nature Geoscience, pp. 339–346, 2013.

Danabasoglu, G.: On multidecadal variability of the Atlantic Multidecadal Overturning Circulation in the Community Climate System Model Version 3, Journal of Climate, 21, 5524–5544, 2008.

Delworth, T. and Mann, M.: Observed and simulated multidecadal variability in the Northern Hemisphere, Climate Dynamics, 16, 661–676, 2000.

Delworth, T., Manabe, S., and Stouffer, R.: Interdecadal Variations of the Thermohaline Circulation in a Coupled Ocean-Atmosphere Model, Journal of Climate, 6, 1993–2011, 1993.

Dijkstra, H., te Raa, L., Schmeits, M., and Gerrits, J.: On the Physics of the Atlantic Multidecadal Oscillation, Ocean Dynamics, 56, 2006.

Dijkstra, H., Frankcombe, L., and von der Heydt, A.: A stochastic dynamical systems view of the Atlantic Multidecadal Oscillation, Philosophical Transactions of the Royal Society A, 366, 2545–2560, 2008.

Dong, B., Sutton, R., and Scaife, A.: Multidecadal modulation of El Nino-Southern Oscillation (ENSO) variance by Atlantic Ocean sea surface temperatures, Geophysical Research Letters, 33, 2006.

Enfield, D., Mestas-Nunez, A., and Trimble, P.: The Atlantic Multidecadal Oscillation and its relation to rainfall and river flows in the continental U.S., Geophysical Research Letters, 28, 2077–2080, 2001.

Friedman, A., Hwang, Y.-T., Chiang, J., and Frierson, D.: Interhemispheric temperature asymmetry over the twentieth century and in future projections, Journal of Climate, 26, 5419–5433, 2013.

Gray, S., Graumlich, L., Betancourt, J., and Pederson, G.: A tree-ring based reconsruction of the Atlantic Multidecadal Oscillation since 1567 AD, Geophysical Research Letters, 31, 2004.

Hakim, G., Emile-Geay, J., Steig, E., Noone, D., Anderson, D., Tardif, R., Steiger, N., and Perkins, W.: The Last Millennium Climate Reanalysis Project: Framework and First Results, Journal of Geophysical Research: Atmospheres, 121, 6745–6764, 2016.

Hakkinen, S., Rhines, P., and Worthen, D.: Atmospheric blocking and Atlantic multidecadal ocean variability, Science, 334, 655–659, 2011.

Hansen, J., Ruedy, R., Sato, M., and Lo, K.: Global surface temperature change, Reviews of Geophysics, 48, 2010.

Hartmann, D.: Global Physical Climatology, vol. 56 of *International Geophysics*, Academic Press, 1994.

Henson, S., Dunne, J., and Sarmiento, J.: Decadal variability in North Atlantic phytoplankton blooms, Journal of Geophysical Research, 114, 2009.

Hetzinger, S., Pfeiffer, M., Dullo, W.-C., Keenlyside, N., Latif, M., and Zinke, J.: Caribben coral tracks Atlantic Multidecadal Oscillation and past hurricane activity, Geology, 36, 11–14, 2008.

Jungclaus, J. et al.: Climate and carbon-cycle variability over the last millennium, Climate of the Past, 6, 723–737, 2010.

Knight, J., Folland, C., and Scaife, A.: Climate impacts of the Atlantic Multidecadal Oscillation, Geophysical Research Letters, 33, 2006.

Knudsen, M., Seidenkrantz, M.-S., Jacobsen, B., and Kuijpers, A.: Tracking the Atlantic Multidecadal Oscillation through the last 8,000 years, Nature Communications, 2, 2011.

Knudsen, M., Jacobsen, B., Seidenkrantz, M.-S., and Olsen, J.: Evidence for external forcing of the Atlantic Multidecadal Oscillation since termination of the Little Ice Age, Nature Communications, 5, 2014.

Kushnir, Y.: Interdecadal Variations in North Atlantic Sea Surface Temperature and Associated Atmospheric Conditions, Journal of Climate, 7, 141–157, 1994.

Landrum, L., Otto-Bliesner, B., Wahl, E., Conley, A., Lawrence, P., Rosenbloom, N., and Teng, H.: Last Millennium Climate and its Variability in CCSM4, Journal of Climate, 26, 1085–1111, 2012.

McCabe, G., Palecki, M., and Betancourt, J.: Pacific and Atlantic Ocean influences on multidecadal drought frequency in the United States, Proceedings of the National Academy of Sciences, 101, 4136–4141, 2004.

McCarthy, G., Haigh, I., Hirschi, J.-M., Grist, J., and Smeed, D.: Ocean impact on decadal Atlantic climate variability revealed by sea-level observations, Nature, 521, 508–510, 2015.

Miles, M., Furevik, D. D. T., Jansen, E., Moros, M., and Ogilvie, A.: A signal of persistent Atlantic multidecadal variability in Arctic sea ice, Geophysical Research Letters, 41, 463–469, 2014.

Morice, C., Kennedy, J., Rayner, N., and Jones, P.: Quantifying uncertainties in global and regional temperature change using an ensemble of observational estimates: the HadCRUT4 dataset, Journal of Geophysical Research: Atmospheres, 117, D08 101, 2012.

Nigam, S., Guan, B., and Ruiz-Barradas, A.: Key role of the Atlantic Multidecadal Oscillation in 20th century drought and wet periods over the Great Plains, Geophysical Research Letters, 38, 2011.

Ottera, O., Bentsen, M., Drange, H., and Suo, L.: External forcing as a metronome for Atlantic multidecadal variability, Nature Geoscience, 3, 688–, 2010.

Parker, D., Legg, T., and Folland, C.: A new daily Central England Temperature Series, International Journal of Climatology, 12, 317–342, 1992.

Peixoto, J. and Oort, A.: Physics of Climate, American Institute of Physics, 1992.

Perkins, W. and Hakim, G.: Reconstructing past climate by using proxy data and a linear climate model, Climate of the Past, (in review), 2016.

Polyakov, I., Bhatt, U., Simmons, H., Walsh, D., Walsh, J., and Zhang, X.: Multidecadal variability of north Atlantic temperature and salinity during the twentieth century, Journal of Climate, 18, 4562–4581, 2005.

R. Lu, B. D. and Ding, H.: Impact of the Atlantic Multidecadal Oscillation on the Asian summer monsoon, Geophysical Research Letters, 33, 2006.

Smith, T., Reynolds, R., Peterson, T., and Lawrimore, J.: Improvements to NOAA's historical merged land-ocean surface temperature analysis (1880-2006), Journal of Climate, 21, 2283–2296, 2008.

Steiger, N., Hakim, G., Steig, E., Battisti, D., and Roe, G.: Assimilation of Time-Averaged Pseudoproxies for Climate Reconstruction, Journal of Climate, 27, 426–441, 2014.

Sutton, R. and Hodson, D.: Atlantic Ocean Forcing of North American and European Summer Climate, Science, 309, 115–118, 2005.

Tandon, N. and Kushner, P.: Does External Forcing Interfere with the AMOC's Influence on North Atlantic Sea Surface Temperature, Journal of Climate, 28, 6309–6323, 2015.

Thomson, D.: Spectrum Estimation and Harmonic Analysis, Proc. IEEE, 70, 1055–1096, 1982.

Torrence, C. and Compo, G.: A Practical Guide to Wavelet Analysis, Bulletin of the Americal Meteorological Society, 79, 61–78, 1998.

Tung, K. and Zhou, J.: Using data to attribute episodes of warming and cooling in instrumental records, Proceedings of the National Academy of Sciences, 110, 2058–2063, 2013.

Vincze, M. and Janosi, I.: Is the Atlantic Multidecadal Oscillation a statistical phantom?, Nonlinear Processes in Geophysics, 18, 469–475, 2011.

Wunsch, C.: The Interpretation of Short Climate Records, with Comments on the North Atlantic and Southern Oscillations, Bulletin of the Americal Meteorological Society, 80, 245–255, 1999.

Zhang, R. and Delworth, T.: Impact of Atlantic multidecadal oscillations on India/Sahel rainfall and Atlantic Hurricanes, Geophysical Research Letters, 33, 2006.

Zhang, R., Delworth, T., and Held, I.: Can the Atlantic Ocean drive the observed multidecadal variability in Northern Hemisphere mean temperature, Geophysical Research Letters, 34, 2007.

Zhang, R., Delworth, T., Sutton, R., Hodson, D., Dixon, K., Held, I., Kushnir, Y., Marshall, J., Ming, Y., Msadek, R., Robson, J., Rosati, A., Ting, M., and Vecchi, G.: Have Aerosols caused the observed Atlantic Multidecadal Variability, Journal of Climate, 70, 1135–1144, 2013.